International Journal of Research in Engineering and Science (IJRES)
ISSN (Online): 2320-9364, ISSN (Print): 2320-9356
www.ijres.org Volume 12 Issue 5 ǁ May 2024 ǁ PP. 303-315

Simulating Influence of Different Mortar types on Performance of Masonry wall

[*1]Miqdad Hussain
[2]Bin Peng
[*1]*School of environment and architecture, University of Shanghai for science and technology, 516 Jungong Road 200093, China*
[2] *School of environment and architecture, University of Shanghai for science and technology, 516 Jungong Road 200093, China*
Corresponding Author: Miqdad Hussain

Abstract
Masonry is a primeval and widely used element in building construction as a symbol of strength, adaptability, beauty, and preserving cultural heritage. The research aims to reveal the impact of different mortar types on the overall performance of masonry walls and their compatibility with masonry units. The study used a concrete damage plasticity constitutive model for numerical simulation by adopting a simplified micro-modelling approach. The study revealed a significant result, as the existing failure mode was noticed in the masonry presented in the literature. Additionally, compatibility between masonry units was deeply analysed in terms of in-plan shear resistance, deformation, stiffness, and ductility. The results revealed that low-strength mortar offers a high in-plan shear resistance compared to walls constructed with high-strength mortar, and high-strength mortar did not result in greater stiffness in the masonry walls. This study highlights the need for additional research on the behaviour of masonry walls constructed with various types of unit's strengths, providing crucial information for improving structure design and preservation.
Keywords: *Numerical Simulation, CDP, Masonry Wall, Mortar*

Date of Submission: 15-05-2024 Date of acceptance: 29-05-2024

I. INTRODUCTION

Masonry walls are an elementary component of building structures across the world, where construction techniques are constantly changing. From the past several decades to the present, masonry has been used as a structural element for strength, flexibility, and elegance. To maintain structural integrity and stability, these walls are considered a critical part of the construction of buildings, bridges, and other infrastructure projects. They are constructed by combining various units (brick, stone) with mortar. Therefore, to understand structural behavior, material optimization, resilience to loading conditions, and the design of structures, it is very important to know how various types of mortar affect the overall performance of masonry when subjected to different loading scenarios.

Walls built with different types of mortar were tested to investigate their in-plan performance, the results showed that the strength of the mortar has a greater impact on the deformation behavior and load-bearing capabilities of masonry walls [1]. [2] negotiated the non-linear behavior of masonry, including failure mode, the strength of unit-mortar relationships, and the behavior of masonry in various loading conditions with different properties of mortar such as strength, stiffness, and bond strength. [3] concluded that numerous factors, such as constitutive material strength, how these materials are divided into the structure, and the behavior of these materials in different loading conditions, can have a significant impact on the structural design of any given structure. Similarly, Qiang Zhou et al. [4] investigated that plastering with high-strength mortar contributes to improvements in the ultimate bearing capacity and ductility of masonry while examining the impact of mortar strength on the masonry structures. Gihad Mohammad et al. [5] concluded that masonry constructed with low-strength mortar started non-linear behavior at a lower stress-strain ratio than that of masonry walls built with high-strength mortar. This phenomenon describes that failure in masonry starts while non-linear behavior starts due to pore collapse or crack propagation in the mortar. In the series of experimental tests by Zengin B, et al. [6], the masonry walls built with various types of mortar were closely examined to evaluate the performance of the wall. The results showed that walls constructed with higher-strength mortar behaved in an unusual pattern, allowing the higher load-bearing capacity with high-strength ductility to continue to function even after experiencing plastic deformation. Additionally, they investigated that the masonry walls built with high-strength masonry provide a higher loading capacity than the walls built with weak mortar. In fact, the interesting point

was that in weak mortar masonry walls, their ductility increased by 21% in contrast to walls built with high-strength mortar. Research led by Anshu Yadav [7] on the structural behavior of masonry walls built with different mortar types revealed that the masonry wall constructed with low-strength mortar had a noticeable propensity to collapse earlier than the wall built with high-strength mortar. Furthermore, the results revealed that there were significant differences in the compressive strength of these walls: walls made with high-strength mortar had a surprising 252% higher compressive strength than weak-mortar masonry walls. This conspicuous variation in structural performance emphasizes that mortar strength plays an important role in masonry construction's resilience and robustness. It also accentuates how crucial it is to choose the suitable type of mortar to guarantee structural stability and resilience.

While numerous studies have explored traditional experimental methods, the adoption of numerical simulation presents a significant advancement in the field, offering numerous advantages. Numerical simulation provides a cost-effective and efficient means of investigation by reducing time and resource requirements. Additionally, numerical simulation provides researchers unprecedented flexibility to manipulate various parameters, such as mortar composition, brick properties, and environmental conditions, with ease. This approach accurately predicts the structural behavior of masonry under various loading conditions, based on different methods such as the finite element method (FEM) [8], [9] the applied element method (AEM) [10], [11], the discrete element method (DEM) [12], [13], and limit analysis [14], [15], [16].

In this work, simplified micro-modeling approaches based on FEM have been used to develop the numerical model of masonry wall. ABACUS software platform is used to perform numerical simulation. The main objective of this research study is to develop numerical model and simulate it to evaluate the structural response of masonry walls with different types of mortar under in-plan loading conditions and compare the performance of these walls in terms of strength, stiffness, and deformation characteristics.

Against this backdrop, our study uses the to contribute to the existing knowledge by performing numerical simulations, as there has been a noticeable increase in interest in developing numerical approaches since the last several years to

Based on FEM and in the framework of the micro-modeling approach, this research uses by employing advanced computational techniques and the concrete damage plasticity model for constitutive modeling to simulate the behavior of a masonry wall under an in-plan horizontal loading condition. This research contributes to the extensive development of more durable, viable, and economical masonry solutions to improve the quality and performance of masonry by understanding how mortar compositions affect structural integrity. Emphasizing the significance of this research, a wide range of studies have been conducted on how mortar types (composition) influence the performance of masonry construction.

Nomenclature

$\boldsymbol{\sigma, \varepsilon}$	Stress and Strain
$\boldsymbol{\varepsilon_0}$	Peak strain
D	Damage evolution
E_b	Elastic modulus (brick)
E_m	Elastic modulus (mortar)
$E_{adj,m}$	Adjusted Elastic modulus (Masonry)
f_{cu}	Peak compressive strength (Concrete)
f_m'	Compressive strength of masonry prism
G_b	Shear modulus of brick
G_m	Shear modulus of mortar
h_m	Thickness of mortar layer
$\mathbf{K}$	Stiffness matrix
K_{nn}	Stiffness of masonry joints (normal direction)
K_{ss}	Stiffness of masonry interfaces (first shear direction)
K_{tt}	Stiffness of masonry interfaces (second shear direction)
D	Variable for damage evolution
$\mathbf{t}$	Nominal stress traction
t_n	stress traction (normal direction)
t_s	stress traction (first direction)
t_t	shear stress traction (second direction)

δ Separation vector
δ_n Separation (normal direction)
δ_s Separation (first direction)
δ_t Separation (second direction)
δ_0 Separation at damage initiation
δ_{cr} Separation at critical damage
τ_n Tensile stress of joints (normal direction)
$\tau_n^{\max}$ Tensile strength of joints (normal direction)
τ_s Shear stress in joints (first shear direction)
$\tau_s^{\max}$ Shear strength in joints (first shear direction)
$\boldsymbol{\tau_t}$ Shear stress in joints (second shear direction)
$\boldsymbol{\tau_t^{max}}$ Shear strength in joints (second shear direction)

II. BRIEF OVERVIEW OF EXPERIMENTAL DATA

To support our research goals, experimental data for this study was taken from the body of current literature. Two different kinds of data were used: the first kind came from studies by Peng et al. [17] and Hemat et al. [18], which were used to validate our numerical model and were partially integrated into the Chinese code [19]. The data presented in Table 1 are used to verify the precision and dependability of our numerical simulations by offering important insights into the behaviour of masonry buildings under different loading scenarios. The second type of data was taken from Valerio et al. [20], specifically chosen to evaluate the performance of masonry walls constructed using various mortar types. Presented in Table 2, these data facilitated a comprehensive analysis of how different mortar compositions affect the structural response of masonry walls. It is significant to note that the development of our numerical model relied on Euro Code 6 [21] Eq. (1) to formulate a combined concrete damage plasticity constitutive model for masonry walls. We sought to guarantee the validity and robustness of our research findings by utilizing experimental data from reliable sources in the field. This would increase the study's credibility and significance in furthering our understanding of the behaviour of masonry walls.

$$f'_m = K \times f_b^{0.85} \quad (1)$$

Where K is equal to 0.45 for general purpose mortar

Table 1: Properties of materials for validation of numerical model.

Material	Elastic Modulus (N/mm^2)	Compressive Strength (N/mm^2)	Tensile Strength (N/mm^2)	Peak Strain	Poisson's Ratio
Brick	7175	6.2	0.62	0.0021	0.15
Mortar	300	1.6	0.16	---	---
Masonry Prism	500	2.12	0.212	0.0021	0.15

Table 2: Properties of Mortar.

Material	Elastic Modulus (N/mm^2)	Compressive Strength (N/mm^2)	Tensile Strength (N/mm^2)
Lime Mortar (Low strength)	192	0.96	0.62
Lime-Cement Mortar (Medium strength)	550	2.75	0.16
Cement Mortar (High strength)	1666	8.33	0.212

III. MODELLING APPROACH

This paper highlights a simplified modeling approach to simulate 3D masonry under concrete damage plasticity as a constitutive model. The thickness of the mortar is added to the units, and joint behavior is modeled as a dis-continuum element. In addition, surface-based cohesion with two yield criteria (tensile and shear) is used to simulate the initial development and propagation of cracks in masonry joints. Two noteworthy aspects of this model are as follows: First, using quasi-static analysis, it allows for an in-depth simulation of the behavior of brick walls under in-plane horizontal loads. Secondly, the suggested model is easy to use and straightforward as it leverages methods readily available in the Abaqus Library without defining user subroutines. Additionally, an analysis of related failure modes included in the models is also stated.

3.1. SURFACE-BASED COHESIVE MODEL

A surface-based cohesive model is employed to simulate the behavior of interfaces along head joints and bed joints of masonry walls where crack initiation, propagation, and interaction occur. These interfaces represent the cohesive behavior of materials, including their tensile strength and shear strength, as well as the energy required for crack propagation. Cracks start to propagate along the interfaces, leading to the failure of masonry when applied loads exceed the cohesive strength of the material.

3.1.1. Response of Joint interfaces in elastic mode

The elastic response of joint interfaces between masonry units (brick and mortar) plays a vital role in finding the overall response of masonry structures. which refers to how these joints contribute to the stiffness of masonry structures when deforming elastically under external loading conditions. This elastic response can be described based on the linear traction separation law, which emphasizes the relationship between loads (traction) and corresponding displacement (separation) Figure 1 before damage forms along joints. This relationship can be expressed by an uncoupled equation for stiffness, which expresses stiffness as a function of the material properties and separation between interfaces at connecting surfaces. This relationship between elastic stiffness (K), nominal traction (t), and relative separation (δ) can be expressed as follows in the matrix form Eq. (2).

$$\begin{bmatrix} t_n \\ t_s \\ t_t \end{bmatrix} = \begin{bmatrix} K_{nn} & 0 & 0 \\ 0 & K_{kss} & 0 \\ 0 & 0 & K_{tt} \end{bmatrix} \begin{bmatrix} \delta_n \\ \delta_s \\ \delta_t \end{bmatrix} \Rightarrow t = K\delta$$

(2)

In simplified micro-model approaches, the stiffness components of joint interfaces in the numerical model should be equal to the original interfaces of masonry under the same boundary conditions. So, the stiffness of masonry joints K_{nn} (normal direction), stiffness of masonry joints K_{ss} (first shear direction), and stiffness of masonry joints K_{tt} (second shear direction) can be determined as the function of elastic moduli of units, mortar and the thickness of mortar layer expressed in Eqs. (3) and (4).

$$K_{nn} = \frac{E_b E_m}{h_m}$$

(3) $$K_{ss}, K_{tt} = \frac{G_b . G_m}{h_m}$$

(4)

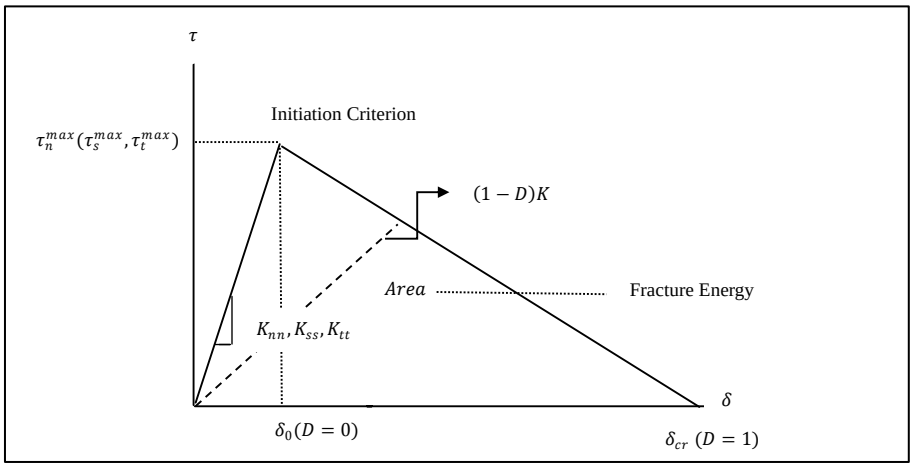

Fig 1: Traction Separation response of interfaces in tension and shear direction

3.1.2. Response of joint interfaces in plastic mode

The joint interface in masonry undergoes plastic deformation when the initial linear response of interfaces exceeds its elastic limit. This response is then followed by crack propagation along masonry joints due to excessive loads. In this paper, the damage initiation is defined using the maximum nominal stress criterion. This criterion is expressed as an elliptic for Eq. (5), where joints are subjected to tensile stress in the normal direction and shear stress in the first and second directions.

$$\left(\frac{\tau_n}{\tau_n^{\max}}\right) + \left(\frac{\tau_s}{\tau_s^{\max}}\right) + \left(\frac{\tau_t}{\tau_t^{\max}}\right) = 1$$

(5)

The shear strength of the masonry interfaces is determined by Eq. (6) presented in (GB 50003-2011) [22].

$$f'_{v,m} = k\sqrt{f_m} \quad (6)$$

Where $f'_{v,m}$ and f_m illustrate shear strength of masonry interface and average compressive strength of mortar, respectively. k is a coefficient associated to masonry material based on different specifications. In this study k is taken as 0.2 for the use of general-purpose mortar.

The propagation of masonry causes stiffness degradation once the damage initiation criterion is met, which changes uncoupled equation of stiffness Eq. (2) to Eq. (7).

$$t = (1-D)K\delta \quad (7)$$

3.2. CONCRETE DAMAGE PLASTICITY

In this study, the CDP constitutive model was used by specifying the stress-strain relationship of masonry under both compression and tension behaviour, which is available at the interface of ABACUS software. CDP is the most used constitutive model to simulate the elastic and plastic behaviour of concrete before complete failure under different loading conditions. The concrete damage plasticity model was first proposed by Lubliner et al. [23] and has been extended by numerous researchers to identify the plasticity yield surface of concrete, including pressure sensitivity, plastic flow rules, and strain hardening. As a quasi-static, brittle material, brick masonry exhibits similar nonlinear behaviour to concrete. So, it can also be adopted to accurately simulate the complex behaviour of brick masonry through the concept of isotropic damaged elasticity combined with isotropic compressive and tensile plasticity to determine the inelastic behaviour followed by Eq. (8).

$$F(\sigma) = \frac{1}{1-\alpha}(\alpha I_1 + \beta\sigma_{\max} + \gamma\sigma_{\max} + \sqrt{3J_2} \quad (8)$$

Where I_1, J_2 and $\sigma_{\max}$ represent initial stress invariant, second stress invariant, and sum of all effective stress in three directions respectively. The $\alpha, \beta, and \gamma$ are dimensionless constant when $\sigma_{\max} = 0$. The Figure 2 demonstrated CDP constitutive model, presented by Lubliner et al. their uniaxial compression and tension behaviour.

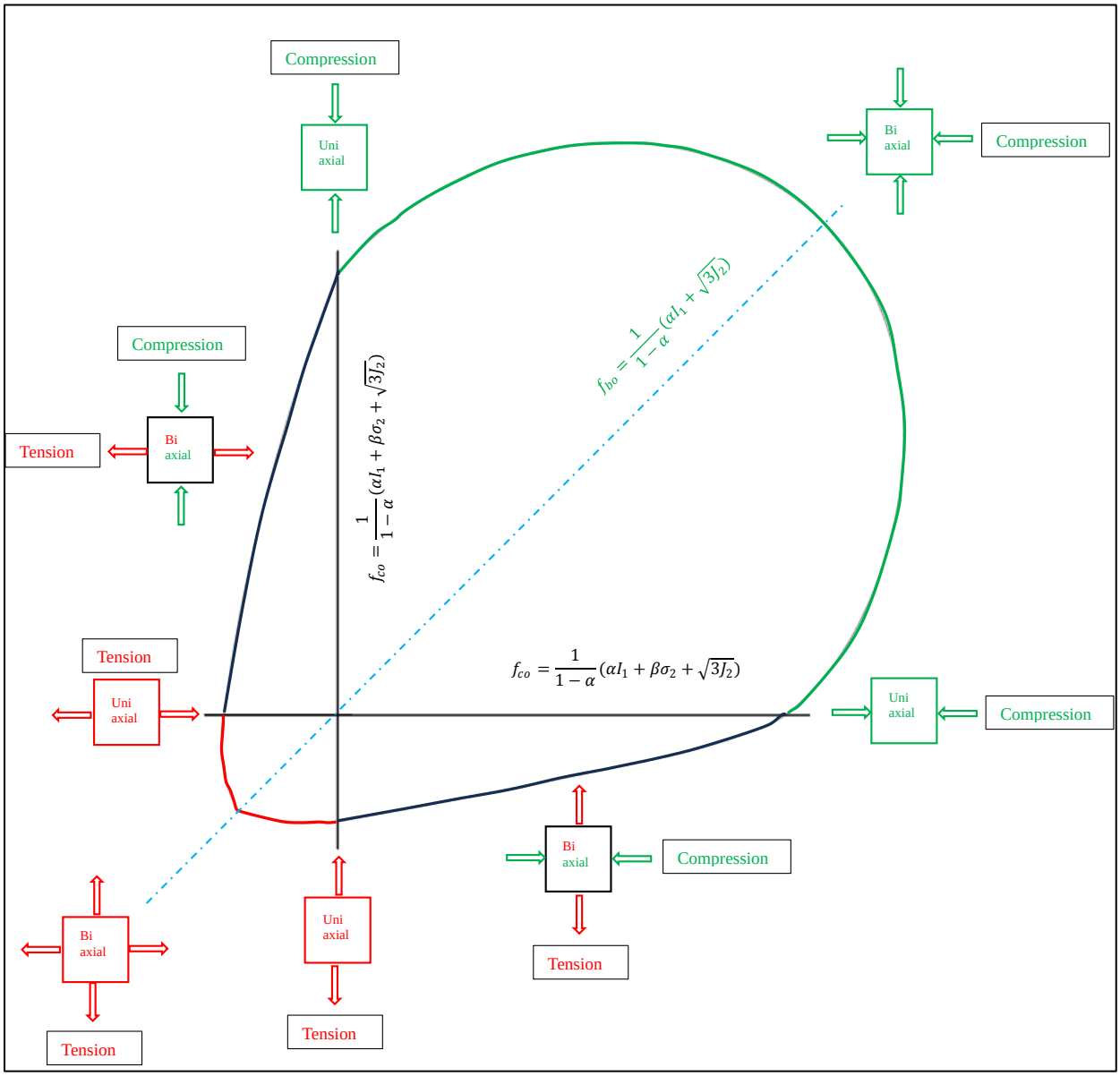

Fig 2: Concrete Damage Plasticity constitutive model [23]

3.2.1. Constitutive Model for Masonry

To define the constitutive model of masonry Eq. (9) ascending part of curve, and Eq. (10) descending part of curve, proposed by Guo and Zhang [24] is used for uniaxial compression stress-strain relationship curve Figure 3.

$$\sigma = \left[\alpha \frac{\varepsilon}{\varepsilon_0} + (3-2\alpha)\left(\frac{\varepsilon}{\varepsilon_0}\right)^2 + (\alpha-2)\left(\frac{\varepsilon}{\varepsilon_0}\right)^3 \right] f_{cu} \quad (9)$$

$$\sigma = \left[\frac{\varepsilon/\varepsilon_0}{\beta\left(\varepsilon/\varepsilon_0 - 1\right)^2 + \varepsilon/\varepsilon_0} \right] f_{cu} \quad (10)$$

Where α represents the ratio between initial tangential modulus E_c and peak secant modulus E_{sec}, normally taken as 1.5 to 3. This paper assumed (α) as 2.2 and (β) as 2 which show the parametric relationship between stress-strain at descending stage of the curve.` The CDP parameter is presented in Table 3.

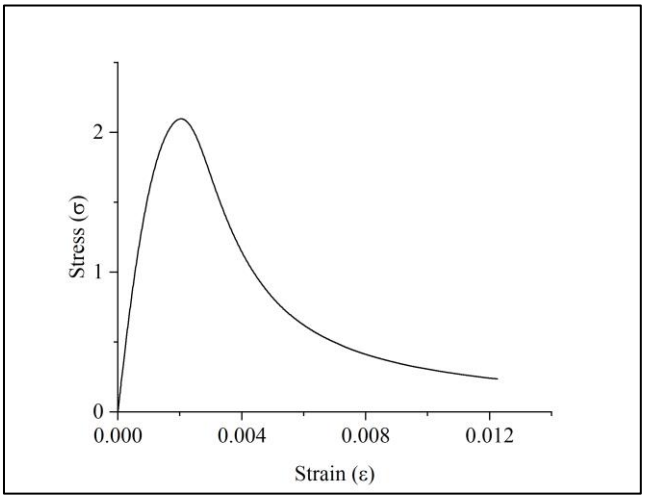

Fig 3: Stress-Strain relationship curve of masonry prism

Table 3: The CDP parameters of Masonry Prism.

Material	Elastic Modulus (N/mm^2)	Plasticity Parameters				
Brick	7175	Dilation angle	Eccentricity	fb_0/fc_0	K	viscosity parameter
		31	0.1	1.16	0.67	0

Brick Compressive Behavior		Brick Compression Damage	
Yield Stress	Inelastic Strain	Damage Parameters	Inelastic Strain
1.240	0	0	0
2.120	0.0014	0	0
1.382	0.0028	0	0
0.840	0.0042	0.286	0
0.578	0.0056	0.3393	0.19193
0.434	0.007	0.3914	0.41179
0.345	0.0084	0.4418	0.55267
0.286	0.0098	0.4914	0.64803
0.244	0.0112	0.5407	0.71552
Brick Tensile Behavior		Brick Tension Damage	
Yield Stress	Cracking Strain	Damage Parameter	Cracking Strain
0.212	0	0	0
0.035333333	0.004028	0.9	0.004028

3.3. MASONRY ASSEMBLAGE ADJUSTED ELASTIC BEHAVIOR

To develop a tantamount elastic response in a numerical model for the experimental masonry assemblage, the elastic modulus of the masonry should be adjusted. It can be determined by taking the compressive strength of the masonry assemblage into consideration. In this study, Eq. (11) proposed by Hemant B. Kaushik et al. [25] is used based on compressive strength, modulus of elasticity and uniform stress distribution between masonry constituents.

$$E_{adj,m} = 250 \times f'_m \quad (11)$$

IV. NUMERICAL MODELLING

The widely available simulation tool "ABACUS" is used to simulate the behavior of masonry walls. To validate numerical model, an eight-nodded hexahedral element with hourglass control and reduced integration (C3D8R type) followed by a simplified micro-modeling approach is used. The interface between units was defined based on a surface-based cohesive approach. The contact between interfaces is defined using surface-to-surface contact (available in Abacus) with a fraction coefficient of 0.7, a zero-slip rate, and neglecting contact pressure. The pressure overclosure behavior of interfaces between masonry constituents is set as "hard contact" by allowing separation of surfaces after contact. This phenomenon results in avoiding surface-to-surface penetration when they are in contact during loading.

The properties of interfaces for different walls are presented in Table 4. The Newton-Raphson method with nonlinear dynamic implicit procedures was used to control the numerical singularity and convergence

issues when solving nonlinear equilibrium equations in each increment during analysis. In-plan lateral load was applied on the top

left of the wall using displacement control procedures. The bottom of the wall was fixed by rigid concrete beam with zero displacement in three directions. The profile of the wall is shown in Figure 4.

Different mesh sizes were adopted based on mesh sensitivity studies. Finally, the (4×1×3 elements) mesh size (60 mm) in Figure 5 is adopted as it showed favourable results for the validation of the model at a lower computational cost. The Chinese standard brick size (240mm lenagth×112mm width×70mm height) is used to model the wall by adding 10mm of mortar layer to the brick as an expended unit. The validation result is presented in Figure 6 in terms of the force displacement relationship. After validation, three walls labelled W-LM (Wall with Lime Mortar), W-CLM (Wall with Cement Lime Mortar), and W-CM (Wall with Cement Mortar) are simulated and compared in terms of ultimate deformation, in-plan shear resistance, stiffness, and ductility. It's important to mention that the compressive strength of brick was kept the same for all walls.

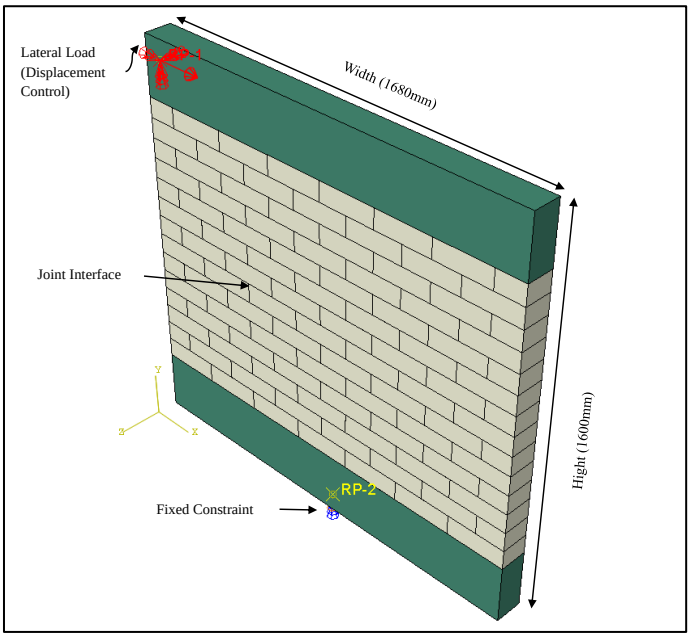

Fig 4: Profile of wall

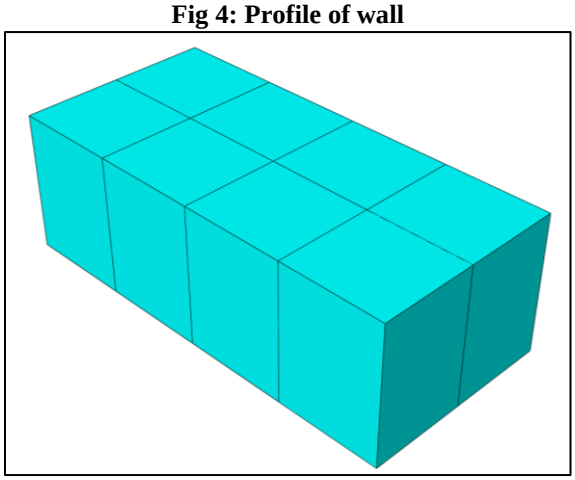

Fig 5: Meshing of element

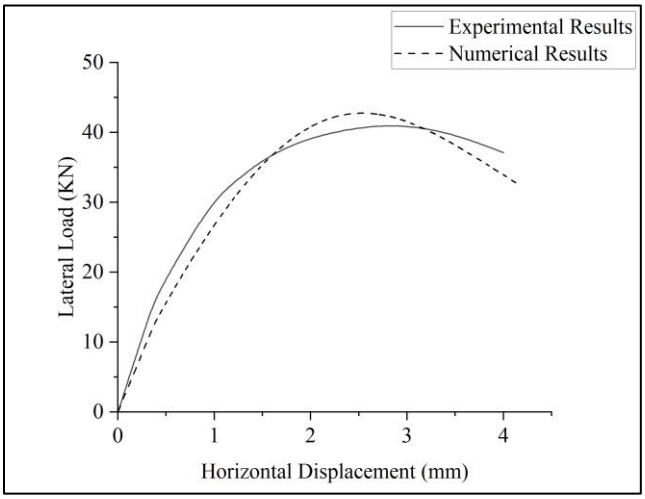

Fig 6: Validation Results in terms of Load-Displacement

Table 4: Properties of interface for walls.

Masonry Wall	K_{nn} (N/mm^3)	K_{ss} (N/mm^3)	K_{tt} (N/mm^3)	Tensile strength in normal direction	Shear strength in first & second direction	Fracture energy
W-LM	19.72	11.7	11.7	0.096	0.19	0.083
W-CLM	59.56	36.1	36.1	0.275	0.33	0.127
W-CM	217	142	142	0.833	0.57	0.213

V. RESULTS AND DISCUSSIONS

5.1. FAILURE AND DEFORMATION

Failure of masonry walls, when subjected to in-plan lateral loading conditions, mainly depends on the shear strength capacity of the masonry. Once load exceeds the shear strength capacity, cracks start to generate and propagate continuously along the head joints, bed joints, and diagonal of the walls. Three main types of failure are presented in the literature, including shear slides at bed joints, diagonal cracking [26] and rocking.

During the analysis of the results, all three types of failure modes Figure 7 were noticed in the masonry walls. Firstly, diagonal cracks formed at the centre of the wall and started to propagate along the corners of the wall. Ultimately, walls failed due to shear slides across horizontal bed joints over the compression corner (rocking). The wall constructed with low-strength mortar (W-LM) resists more ultimate deformation than the wall built with high-strength mortar. The tensile stress concentration becomes visible (at 0.5mm displacement) at the centre with loads of 17.4KN, 13.4KN, and 18.6KN at walls W-LM, W-CLM, and W-CM, respectively. The results indicate that the wall constructed with low strength mortar showed better compatibility with bricks in terms of compressive strength. The presence of high compressive strength mortar in wall W-LCM and W-CM leads to brittle behaviour at interfaces due to stress concentration (because of mismatch of material), which results in premature failure of the wall under low external loads. The ultimate deformation of a wall constructed with low-strength mortar was 11% higher than that of a wall constructed with high-strength mortar. The comparison is shown in Figure 8.

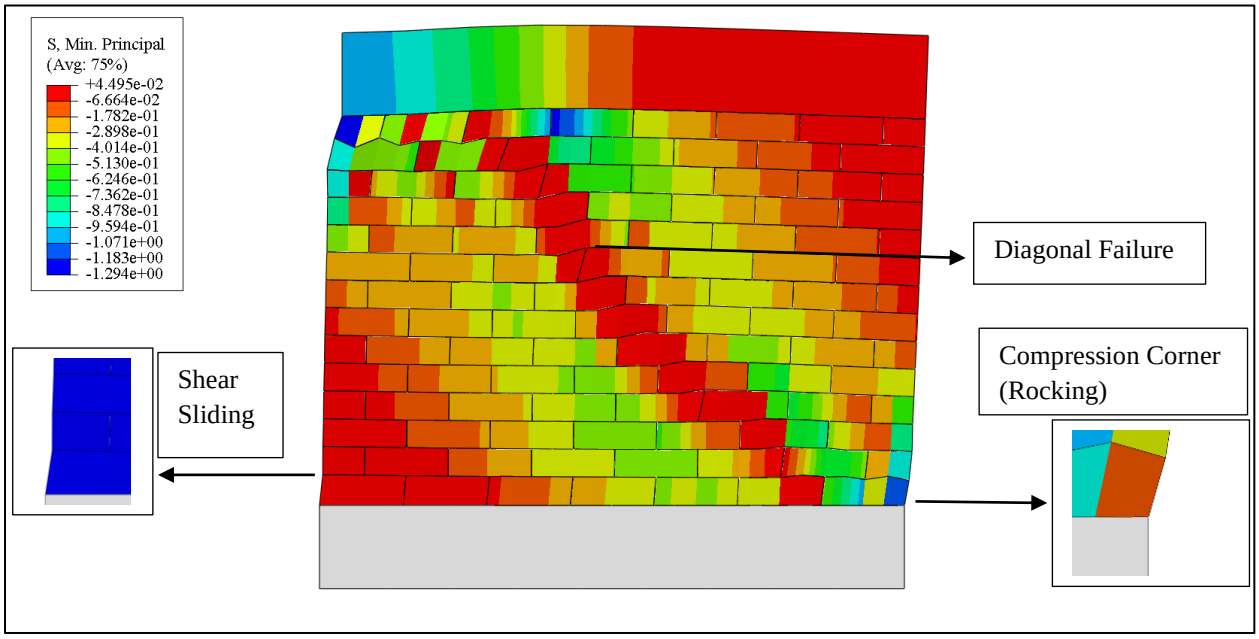

Fig 7: Failure mode of walls (scale factor 15)

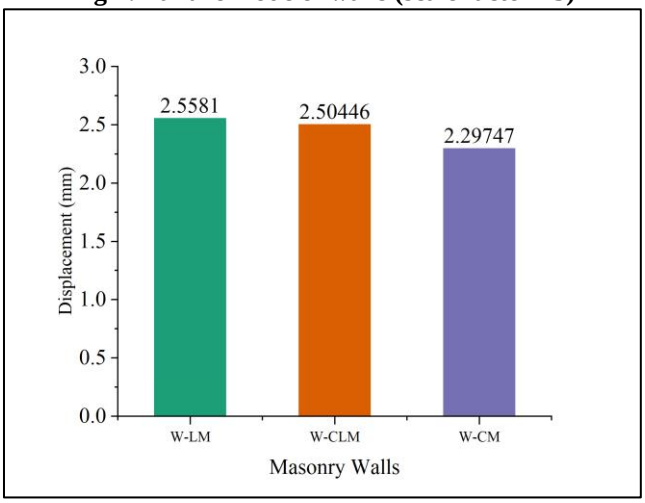

Fig 8: Comparison of walls in term of deformation

5.2. IN-PLAN SHEAR RESISTANCE AND STIFFNESS

While analysing the in-plan shear resistance, we noticed unexpected results, where masonry wall constructed with low-strength mortar (W-LM) offer greater in-plan shear resistance compared to other walls. As in the case of a masonry wall, units (bricks and stones) serve as a primary load-bearing element, while mortar acts as a binding agent, distributing stresses along the wall and improving its stability. So, as the results above indicate, the in-plan shear resistance of masonry is not only dependent on the compressive strength of mortar; however, its binding properties, flexibility, and compatibility with units also play a vital role in distributing loads and resisting shear forces across the masonry. The in-plan shear resistance of W-LM was 37% greater than that of W-LCM and 5% greater than that of W-CM (high-strength mortar). Figure 9 shows the comparison of walls in terms of force displacement relationships.

There was not any significant change in stiffness across the walls. However, the wall constructed with medium strength (W-CLM) provides minimum stiffness compared to other walls Figure 10.

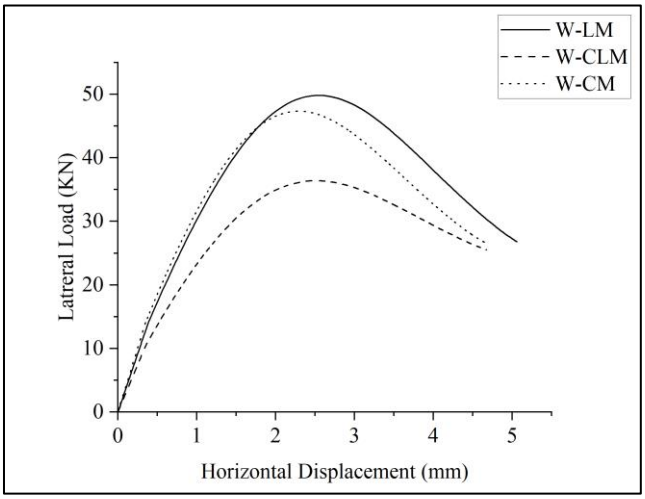

Fig 9: Comparison of walls in terms of Load-Displacement

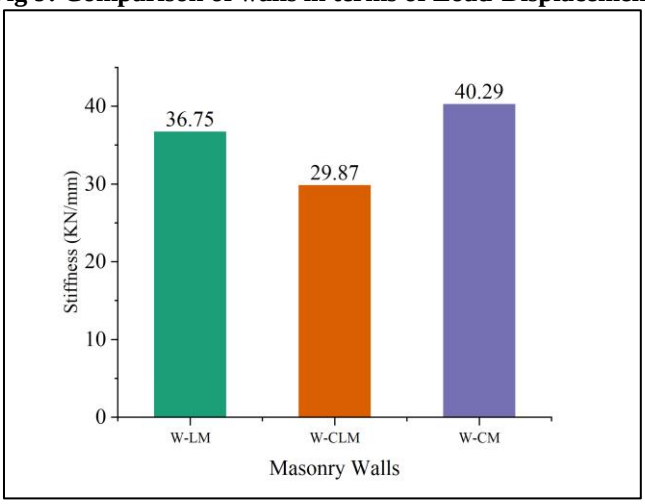

Fig 10: Comparison of walls in term of stiffness

5.3. DUCTILITY

In this study Eq. (12) is used to evaluate ductility using displacement ductility coefficient.

$$u = \Delta_u / \Delta_y \quad (12)$$

Where u, Δ_u and Δ_y represent displacement ductility coefficient, ultimate displacement, and yield displacement, respectively. There are several definitions presented in the literature for the point of ultimate and yield displacement based on various laboratory tests. In this study, the yield displacement is taken at the point corresponding to 75% of the ultimate load in the ascending curve, while the ultimate point is taken as the displacement corresponding to the ultimate load. Figure 11 presents the displacement ductility coefficient of walls. The results indicated that there was no significant change in ductility as the compressive strength of bricks remained unchanged across all walls. This indication provides an argument that crack propagation and deformation in masonry have been mainly controlled by bricks.

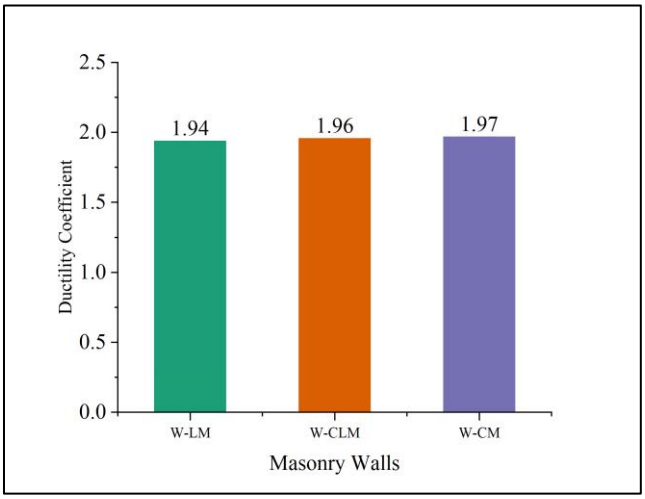

Fig 11: Comparison of walls in term of ductility

VI. CONCLUSION

Our research highlights the complex interactions that exist between mortar characteristics, unit properties, and masonry performance.

- The behaviour of masonry structures with multiple kinds of mortar can be accurately simulated by employing the concrete damage plasticity constitutive model. This sophisticated modelling approach made it possible to thoroughly investigate how mortar properties affect masonry performance.
- Our findings highlight the significance of mortar-unit compatibility in masonry wall in-plan shear resistance analyses as the wall constructed with low strength mortar offer a high in-plan shear resistance compared to walls constructed with high strength mortar. Although the mortar's and units' compressive strengths are significant, the compatibility of these materials has a more significant effect on how stress is distributed throughout the wall. This emphasizes how important it is to take into consideration the mechanical interaction between mortar and units when constructing and designing masonry.
- High-strength mortar did not result in greater stiffness in the masonry walls. Rather, a decrease in stiffness was caused by the concentration of stress at the interface between the two materials.
- No significant variations in ductility were found across the walls, despite variations in mortar strength. This emphasizes how important bricks are for preventing cracks from spreading and preserving structural integrity

Statement

On behalf of all authors, the corresponding author states that there is no conflict of interest.

REFERENCES

[1] Y. Peng, G. Zhao, Y. Qi, and Q. Zeng, "In-situ assessment of the water-penetration resistance of polymer modified cement mortars by μ-XCT, SEM and EDS," Cem Concr Compos, vol. 114, Nov. 2020, doi: 10.1016/j.cemconcomp.2020.103821.

[2] E. L. Woen, M. A. Malek, B. S. Mohammed, T. Chao-Wei, and M. T. Tamunif, "Experimental study on compressive strength of sediment brick masonry," in AIP Conference Proceedings, American Institute of Physics Inc., Feb. 2018. doi: 10.1063/1.5022911.

[3] K. R. C. Andrzej S. Nowak, Reliability of Structures, 2nd ed. New York: CSC Press, 2019.

[4] Q. Zhou, L. Yang, and W. Zhao, "Experimental Analysis of Seismic Performance of Masonry Shear Wall Reinforced with PP-Band Mesh and Plastering Mortar under In-Plane Cyclic Loading," Advances in Civil Engineering, vol. 2020, 2020, doi: 10.1155/2020/4015790.

[5] G. Mohamad, F. S. Fonseca, A. T. Vermeltfoort, D. R. W. Martens, and P. B. Lourenço, "Strength, behavior, and failure mode of hollow concrete masonry constructed with mortars of different strengths," Constr Build Mater, vol. 134, pp. 489–496, Mar. 2017, doi: 10.1016/j.conbuildmat.2016.12.112.

[6] B. Zengin, B. Toydemir, S. Ulukaya, D. Oktay, N. Yüzer, and A. Kocak, "The effect of mortar type and joint thickness on mechanical properties of conventional masonry walls," Structural Engineering and Mechanics, vol. 67, no. 6, pp. 579–585, Sep. 2018, doi: 10.12989/sem.2018.67.6.579.

[7] A. Yadav and S. Pal, "The impact of mortar thickness and strength on the brick masonry prism: An investigation," in Materials Today: Proceedings, Elsevier Ltd, 2023, pp. 552–559. doi: 10.1016/j.matpr.2023.10.035.

[8] L. Macorini and B. A. Izzuddin, "A non-linear interface element for 3D mesoscale analysis of brick-masonry structures," Int J Numer Methods Eng, vol. 85, no. 12, pp. 1584–1608, Mar. 2011, doi: 10.1002/nme.3046.

[9] S. Zhang, S. M. Taheri Mousavi, N. Richart, J. F. Molinari, and K. Beyer, "Micro-mechanical finite element modeling of diagonal compression test for historical stone masonry structure," Int J Solids Struct, vol. 112, pp. 122–132, May 2017, doi: 10.1016/j.ijsolstr.2017.02.014.

[10] D. Malomo and A. Penna, "Applied Element modelling of the dynamic response of a full-scale clay brick masonry specimen with flexible diaphragms," 2019. [Online]. Available: https://www.researchgate.net/publication/333811832

[11] R. Soti and A. R. Barbosa, "Experimental and applied element modeling of masonry walls retrofitted with near surface mounted (NSM) reinforcing steel bars," Bulletin of Earthquake Engineering, vol. 17, no. 7, pp. 4081–4114, Jul. 2019, doi: 10.1007/s10518-019-00607-2.
[12] B. Pulatsu, E. M. Bretas, and P. B. Lourenço, "Discrete element modeling of masonry structures: Validation and application."
[13] M. Pepe, M. Pingaro, E. Reccia, and P. Trovalusci, "MICROMODELS FOR THE IN-PLANE FAILURE ANALYSIS OF MASONRY WALLS WITH FRICTION: LIMIT ANALYSIS AND DEM-FEM/DEM APPROACHES," 2019.
[14] L. Cascini, R. Gagliardo, and F. Portioli, "LiABlock_3D: A Software Tool for Collapse Mechanism Analysis of Historic Masonry Structures," International Journal of Architectural Heritage, vol. 14, no. 1, pp. 75–94, Jan. 2020, doi: 10.1080/15583058.2018.1509155.
[15] S. Tiberti and G. Milani, "3D homogenized limit analysis of non-periodic multi-leaf masonry walls," Comput Struct, vol. 234, Jul. 2020, doi: 10.1016/j.compstruc.2020.106253.
[16] M. Breccolotti, L. Severini, N. Cavalagli, F. M. Bonfigli, and V. Gusella, "Rapid evaluation of in-plane seismic capacity of masonry arch bridges through limit analysis," Earthquake and Structures, vol. 15, no. 5, pp. 541–553, Nov. 2018, doi: 10.12989/eas.2018.15.5.541.
[17] B. Peng, S. Wei, L. Long, Q. Zheng, Y. Ma, and L. Chen, "Experimental investigation on the performance of historical squat masonry walls strengthened by UHPC and reinforced polymer mortar layers," Applied Sciences (Switzerland), vol. 9, no. 10, May 2019, doi: 10.3390/app9102096.
[18] H. B. Kaushik, ; Durgesh, C. Rai, S. K. Jain, and M. Asce, "Stress-Strain Characteristics of Clay Brick Masonry under Uniaxial Compression", doi: 10.1061/ASCE0899-1561200719:9728.
[19] Y. Zhenfang and L. Bin, "A BRIEF INTRODUCTION TO A NEWLY REVISED VERSION OF THE CHINESE CODE FOR DESIGN OF MASONRY STRUCTURES (GB50003-2001)."
[20] V. Alecci, M. Fagone, T. Rotunno, and M. De Stefano, "Shear strength of brick masonry walls assembled with different types of mortar," Constr Build Mater, vol. 40, pp. 1038–1045, 2013, doi: 10.1016/j.conbuildmat.2012.11.107.
[21] "EN 1996-1-1: Eurocode 6: Design of masonry structures - Part 1-1: General rules for reinforced and unreinforced masonry structures," 2005.
[22] "NATIONAL STANDARD OF THE PEOPLE'S REPUBLIC OF CHINA 中华人民共和国国家标准 Code for Design of Masonry Structures Jointly Issued by the Ministry of Housing and Urban-Rural Development of the People's Republic of China and the General Administration of Quality Supervision, Inspection and Quarantine of the People's Republic of China."
[23] J. Lubliner, S. A. O. S. Oller, and E. O%ate, "A PLASTIC-DAMAGE MODEL FOR CONCRETE."
[24] Z. X. Z. D. W. R. Guo Zhenhai, "Experimental Investigation of the Complete Stress-Strain Curve of Concrete," Journal of Building Structures, vol. 03, no. 01, pp. 1–12, Feb. 1982.
[25] H. B. Kaushik, ; Durgesh, C. Rai, S. K. Jain, and M. Asce, "Stress-Strain Characteristics of Clay Brick Masonry under Uniaxial Compression", doi: 10.1061/ASCE0899-1561200719:9728.
[26] F. Cakir, E. Uckan, J. Shen, B. S. Seker, and B. Akbas, "Seismic damage evaluation of historical structures during Van earthquake, October 23, 2011," Eng Fail Anal, vol. 58, pp. 249–266, Dec. 2015, doi: 10.1016/J.ENGFAILANAL.2015.08.030.